PREDICTIVE MICROFLUIDIC MODELING OF PROSTATE TISSUE DIFFERENTIATION DYNAMICS

Adriana ZAINEA[1], Grațiela GRĂDIȘTEANU PÎRCĂLĂBIORU[2,3], Elena-Iuliana BÎRU[2,4], Horia IOVU[2,5]

Nowadays, prostate cancer is a common and life-threatening condition in men. Despite medical advances, treatment remains challenging due to limited understanding of cellular interactions. This study highlights the role of epithelial differentiation in maintaining a healthy prostate environment and aims to develop a prostate-on-a-chip model to better study cellular interactions and improve diagnostics and preventive therapy. The simulations indicated a comparable concentration profile when epithelial cells were in both the upper and lower channels, however, the central channel showed a decreasing concentration gradient (from $2.5x10^{-3}$ mol/m^3 to $1.25x10^{-3}$ mol/m^3) at the outlet. Furthermore, the simulations used diffusion coefficients of 2.368 m²/s for collagen and 0.571 m²/s for the epithelial layer. In parallel, PrECs were kept under microfluidic conditions for 48 hours, during which LDH levels rose from 0.06 on day 1 to 0.1 on day 6. Experimental observations showed an enhanced migration toward the central channel when epithelial cells were placed in the upper channel and fibroblasts in the lower channel, while a decrease in migration was noted when epithelial cells filled both channels. In summary, both simulations and experiments demonstrated that channel occupancy is associated with changes in concentration gradients and cell migration.

Keywords: cellular differentiation, microfluidics, prostate cancer, organ-on-a-chip.

1. Introduction

Being one of the most common cancer diagnoses among men, prostate cancer represents the 5th leading cause of death for this group of people.[1] Through the factors that can instigate its appearance, the genetic material, age, diet of the

[1] PhD, Advanced Polymer Materials Group, National University of Science and Technology POLITEHNICA Bucharest, Romania, e-mail: adriana.zainea@upb.ro
[2] Center of Excellence in Bioengineering – eBio-hub, National University of Science and Technology POLITEHNICA Bucharest - CAMPUS, 6 Iuliu Maniu Boulevard, 061344, Bucharest, Romania
[3] Research Institute of the University of Bucharest (ICUB), University of Bucharest, Romania, e-mail: gratiela.gradisteanu@icub.unibuc.ro
[4] Assoc. Prof., Advanced Polymer Materials Group, National University of Science and Technology POLITEHNICA Bucharest, Romania, e-mail: iuliana.biru@upb.ro
[5] Prof., Advanced Polymer Materials Group, National University of Science and Technology POLITEHNICA Bucharest, Romania, e-mail: horia.iovu@upb.ro

individual, certain drugs (e.g., 5-alpha reductase inhibitor), as well as some particular unhealthy habits such as smoking or alcohol consuming are considered to highly impact its evolution. [2], [3]

Since the discovery of prostate-specific antigen (PSA), the prostate cancer is now possible to be identified before it becomes palpable during rectal examination.[4]

Radiotherapy and surgery advancements have lowered side effects and improved cure rates, making routine prostate cancer screening less appealing due to a lack of evidence of quality-of-life advantages. Screening decisions must also take into account potential problems, such as therapies for metastatic cancer, infertility, incontinence, and the discovery of malignancies that may never cause symptoms or shorten life.[5], [6]

The complex anatomy of the prostate makes selecting or developing effective treatments challenging. Its function relies on ducts and acini within the stroma, supported by a layer of columnar epithelium over basal cells forming the basement membrane. The extracellular matrix, connected to stromal cells like smooth muscle myocytes, is vital for contractility and preventing fluid stagnation. Fibroblasts in the stroma also play a key role in supporting the adult prostate ducts.[7]

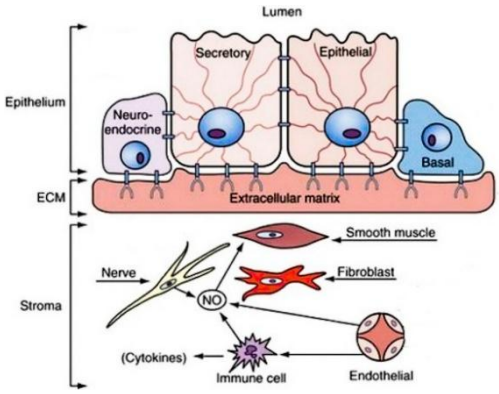

Fig. 1. Schematical representation of full cellular differentiation in the prostate.[8] Copyright 2013, Molecular Endocrinology.

In light of this, currently, only one conclusion has been put forward: the key to the answer lies in the biological interaction between the prostate's stromal and epithelial cells.

This remark arose since the discovery of reactive stroma appearance following epithelial alterations[9]. Furthermore, stromal cells within cancer tissue

may impact epithelial modification by secreting several paracrine substances altering stromal cells, cancer cells, and healthy epithelia. Finally, current studies indicate that irreversible genetic alterations in stromal cells may occur before tumour formation.[10]

Despite this fundamental knowledge, many therapies have been tried out, but a highly fascinating one that has captivated the interest of all in recent years is the *organ-on-a-chip* method. [11], [12]

This curiosity is, however, not spontaneous, finding alternatives to animal testing gains tremendous inquisitiveness because the standard procedures' expensiveness, time-consuming, and morally questioning data often do not accurately predict the outcomes of human clinical trials.[13]

The concept focuses on the two premises that cells grow within the device's channels and chambers advancing the tissue or organ growth to mimic the biology and physiology, and that to perform efficiently, the system must incorporate optimal circumstances related to flow rate, pressure, temperature, pH, nutrient content, osmotic pressure, the presence of toxins, and more.[14]

Moreover, this microfluidic device can carefully keep in control and track in real-time every experiment.[15]

For these reasons, the MIMETAS OrganoPlate® 3-Lane, a commercial microfluidic device, was selected in this investigation. This static 3D microfluidic device allows cell growth in ECM-filled, spatially segregated channels and without active flow[16]. This technology, compared to traditional 2D cultures, provides a three-dimensional microenvironment that promotes e.g., cell-ECM interactions and tissue-like structure. In contrast to traditional 3D co-culture models, the microfluidic design allows for the controlled spatial arrangement of distinct cell types within defined channels, allowing for reproducible cell-cell interactions within physiologically realistic geometrical constraints.[17]

Contrasting previous prostate-on-chip systems, which allowed for long-term coculture to study basal-to-luminal differentiation and glandular morphogenesis, this study focuses on epithelial-stromal interactions within a spatially controlled microfluidic design, employing specific channel configurations and gradients to precisely investigate cell behavior [18].

Earlier approaches used porous membranes to replicate paracrine signaling in the prostate, but they did not investigate how stromal fibroblasts influence epithelial growth, adhesion, differentiation, and directed migration under various channel occupancies and simulated microenvironmental gradients.[19]

The unique feature of our platform is the controlled spatial separation of cell types and the incorporation of simulation-derived gradients, which allow for a quantitative comparison of diffusion profiles with experimentally observed epithelial responses to stromal presence within the prostate-on-chip system.

Therefore, the final aim is to leverage the information about stromal-epithelial interaction in the prostate under the organ-on-a-chip conditions to mimic a biological environment that will be able to assist future treatments for prostate cancer.

2. Experimental section

2.1. Materials

Throughout the study, a variety of materials have been used, such as PrEc-Human Prostate Epithelial Cells and its respective media PrEGM- Prostate Growth Medium BulletKit that contains PrEBM Basal Medium (CC-3165) and PrEGM SingleQuots Supplements, all procured from BioZyme Company, Romania.

Other cell lines used were HDFa (human dermal fibroblasts) and HT-29 (human colorectal adenocarcinoma with epithelial morphology) with their respective media. These substances were a kind donation from Prof. Nicolae Corcionivoschi from Agri-Food and Bioscience Institute Belfast, Northern Ireland.

The Trypsi/EDTA and trypsin neutralizing solution (TNS) were purchased from Lonza, USA.

For the Lactate dehydrogenase assay the reagents used (calcein AM, ethidium homodimer 1) were acquired from Life Technologies Corporation, US. The phosphate-buffered saline (PBS 10x) was purchased from Corning, USA.

Lastly, the platform used for the experiments was OrganoPlate-3Lane from Mimetas Company, Holland.

2.2. Methods

2.2.1. Process Simulations

A series of simulations of fluid flow under various conditions were performed using COMSOL Multiphysics, with the Laminar Flow Interface applied to model slow, stable flows without sudden changes in temperature, shape, or material. The Navier-Stokes equations were solved without a turbulence model, as laminar flow occurred at Reynolds numbers below 1000, and density was assumed constant to represent incompressible flow. Integrating COMSOL helps optimize biological experiments by predicting concentration gradients and diffusion, guiding

channel design and cell seeding, and enabling more efficient cell culture while saving time and resources.

Velocity

To examine the velocity of a fluid in COMSOL simulation, the first important step is to prove the validity of the model, and one can do that by depicting no velocity at the border of every channel, which in this case is confirmed. The blue line among the edges of every margin represents the velocity equal to zero (Fig. 2).[20]

Subsequently, an aspect with great influence to be considered is the cell migration velocity amid shear stress variations because it is the usual approach for studying cell-substrate adhesion, since the differences may also suggest changes in adhesion strength.[21]

As expected, the high and stable velocity levels that the inlets of the microfluidic device can be observed from Fig. 2 as a result of material injection.

Nevertheless, even though the fluid presents itself with steady velocity across most of the middle channel, it shows an increase near the exit. For this situation, it was considered that the contribution of collagen highly influences the migration because it has a diffusion coefficient different from that of the inserted species [22], [23] and therefore, some changes regarding the boundary conditions must be made.

Pressure

For the pressure distribution model, we can see in Fig. -B that in this configuration, the pressure is consistent along each channel, indicating an elevation solely at the inlets.

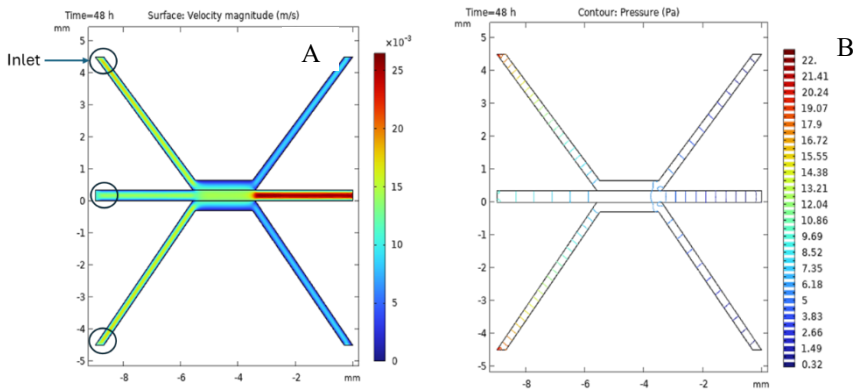

Fig. 2. Velocity (A) and pressure (B) gradient simulations for the parameters set for OrganoPlate 3-lane.

According to the literature, the reason for this is the need for a high boost to spare the injected fluid from being clogged and to permit a constant and smooth flow through the microfluidic device.[24]

Concentration

Because the microfluidic device now contains species of different concentrations, it majorly affects the diffusion in the channels and the cell contact, therefore affecting the concentration model also. Besides this, the coefficient of diffusion is different as well. While collagen has 2.368 $m^2ms^{-1,}$ the epithelia have 0.571 m^2ms^{-1}[25]. Fig. 3 shows a constant, uniform distribution when epithelial cells occupy both upper and lower channels. In the middle channel, the concentration gradient starts high and gradually decreases near the exit. This pattern results from diffusion, which is especially noticeable here due to the high diffusion coefficient of the species.

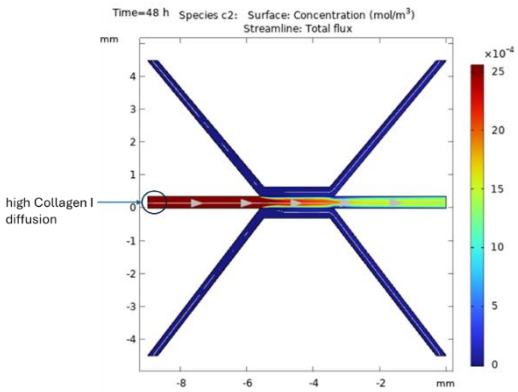

Fig. 3. Concentration gradient simulations for the parameters set for OrganoPlate 3-lane.

2.2.2. Differentiation of the prostate epithelia in the absence of stroma

Regarding the differentiation of epithelial cells, the main impediment was finding out if it was conceivable in terms of microfluidic devices. Because of that, PrECs were cultured in a microchannel using the settings specified in Table 1.

Table 1

Co-culturing of diverse cellular lines to prove epithelial differentiation.

Well	Upper Channel	Bottom Channel
A2	Prostate epithelial cells (PrEc)	Prostate epithelial cells (PrEc)
B2	Prostate epithelial cells (PrEc)	Skin fibroblast cells (HDFa)
B1	Intestine epithelial cells (IEc /HT-29)	Skin fibroblast cells (HDFa)

In the 3-lane OrganoPlate, PrEc were cultured with supportive cells to assess their growth requirements. HT29 intestinal epithelial cells provided epithelial-derived cues, while HDFa fibroblasts offered stromal support. This setup allows investigation of whether PrEc cells require interactions with both epithelial and stromal cells to proliferate and differentiate.

2.2.3. Preparation of the collagen I solution that will serve as ECM gel

According to the MIMETAS protocol, a mixture of 1M HEPES, 37 g/L $NaHCO_3$, and Collagen I, in a ratio of 1:1:8 (%V/V) has to be done to synthesize the ECM gel. Therefore, a solution of 100 mL of ECM gel was prepared with 10 mL of 1M HEPES, 10 mL of $NaHCO_3$, and 80 mL of collagen I.

After this, each inlet in each well was injected in the center with 2.5 mL gel with 30 mL of PBS to avoid the drying of the gel afterward.

2.2.4. Preparation of the cellular lines

In this work, three cellular lines were put into use: prostate epithelial cells (PrEc), prostatic fibroblast cell line (HDFa), and epithelial cells from the intestine (IEc). After the PrEc had sufficiently developed, the subsequent procedures were done to get the highly concentrated pellet required to carry out the study:

1. Removal of the cell culture medium from one of the vessels.
2. Use of 5 mL at room-temperature HEPES-BSS to wash the cells.
3. Extraction of the HEPES-BSS from the flask.
4. Dosing the cells with 2 mL of a 0.25 percent trypsin-EDTA mixture.
5. Trypsinization, that should be continued for two to six minutes, depending on the cell specie, or until around 90% of the cells have rounded up.
6. Release the majority of the cells from the culture surface by tapping the flask on hand. Nevertheless, there is a risk of not allowing enough time for the cells to trypsinize if only a portion of them separate, in which case a pause for 30 seconds should happen before rapping again. The tapping is repeated after a 30-second break if the cells still won't split.
7. Once the cells have been detached, a neutralization of the trypsin in the flask using 4 ml of room-temperature TNS (trypsin neutralization solution) should be done. If a large fraction of the cells does not detach after 7 minutes, the trypsin is most likely too cold or inactive to release them.
8. Transfer of the isolated cells to a sterile 15 mL centrifuge tube.
9. To retrieve any remaining cells, there should be added 2 mL of HEPES-BSS to wash the flask to the centrifuge tube.
10. Examination of the flask containing the gathered cells under a microscope to ensure that the harvest was successful by determining the number of cells that were not eliminated. This should be below 5%.

11. To pellet the cells, centrifugation at 220 x g for five minutes must be performed, followed by:

-aspiration of most of the supernatant, reserving 100–200 mL for yourself.

-gentle flip the cryovial by finger to release the pellet.

12. Determination of the total volume of the cell suspension after diluting it with 2-3mL of growth media.

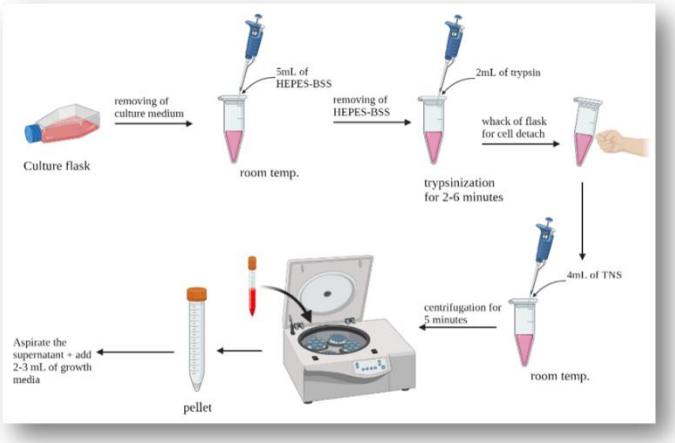

Fig. 4. Schematic representation of steps from 1-12.

13. Cell count with a hemocytometer and trypan blue.

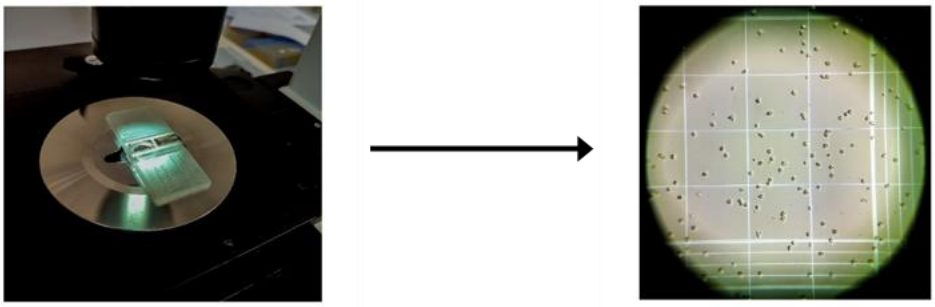

Fig. 5. Cell count setup with effective results.

14. If necessary, another dilution of the solution with HEPES-BSS to achieve the desired cell count per milliliter may proceed subsequently, the cell count also.

2.2.5. Optimization of the injection volumes for the wells

When establishing the experimental setup, all component volumes were calculated using the MIMETAS OrganoPlate 3-Lane channel dimensions.

Although the specific microchannel dimensions and cross-sections are proprietary, all operations followed the manufacturer's instructions to assure adequate channel filling, consistent cell seeding, and stable culture conditions. In this case, after several tests sample quantities were chosen as presented in Fig. 6 where a close look can be taken on the injection process in the wells:

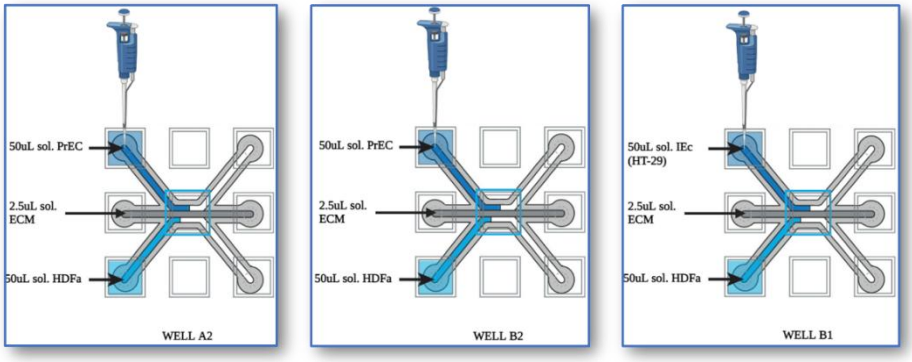

Fig. 6. Schematical representation of well injection optimization.

2.2.6 Characterization techniques

The cell lines were cryopreserved using the ultrafreezer U250 from NORDIC LAB, Denmark. The CB(E3) incubator from Binder GmbH, Germany was used for culturing the cell lines. The lactate dehydrogenase assay was carried out using the NanoQuant Infinite M200PRO from TECAN in Switzerland. The microscopy investigation was conducted using a ZEISS Axio Scope A1 from Germany.

3. Results & Discussion

3.1. Phase contrast observations for prostate epithelia well.

Living, untainted microscopic elements are apparent via phase contrast. Usually, the refractive index variation among a live tiny structure and its surroundings is so narrow that the structure refracts only a small amount of light. The specie, on the other hand, diffracts light. This feature is particularly important for organisms that are still alive, and, therefore, cell culture systems are now the principal material for phase contrast.[26]

These factors led to the use of phase contrast microscopy to investigate the shape and activity of cellular structure, which may be observed by this technique, including invasion and migration.[27]

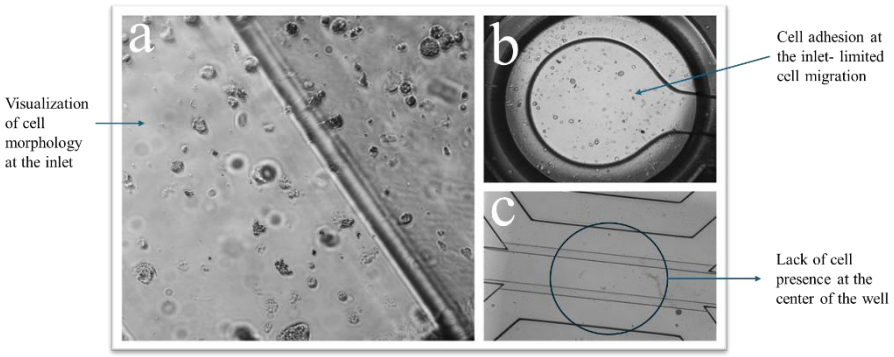

Fig. 7. Imaging performed directly after the seeding of cells via phase contrast microscopy.

In Fig. 7, upon the cells' insertion into the well, an inherent tendency to remain set in place (7b) was seen, along with a significant distance around them. Beyond that, due to the slow development of the cells in optimal conditions, there is a lack of epithelial cells moving near the core (7c) of the well. These factors led to the use of phase contrast microscopy to investigate the shape and activity of cellular structure, which may be observed by this technique, including invasion and migration.

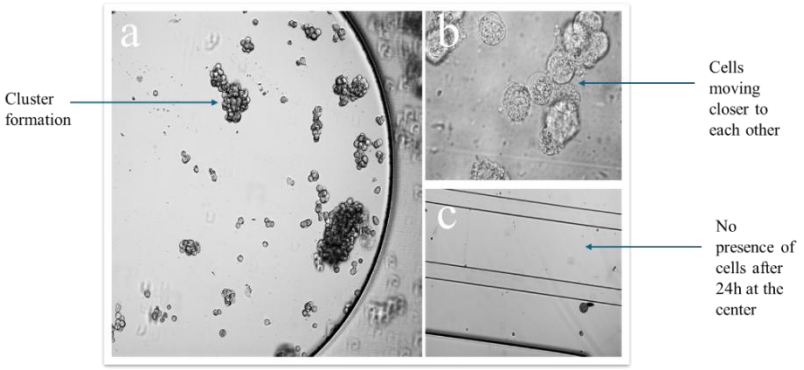

Fig. 8. Imaging performed 24h after the seeding of cells via phase contrast microscopy.

In Fig. 8, the matter seems to be turning better 24 hours post-seeding, signaling that the cells are shifting closer to each other but not enough to get into the ECM route (8c). Moreover, we can see that the cells prefer to grow into clusters (8a;8b).

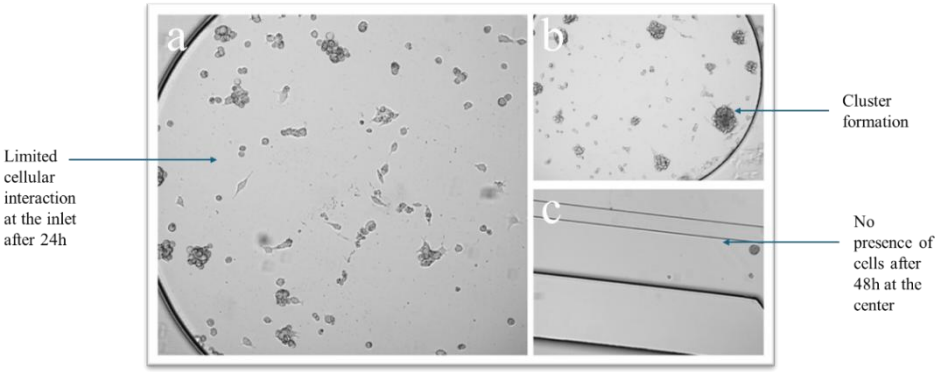

Fig. 9. Imaging performed 48h after the seeding of cells via phase contrast microscopy.

At the end of this part, not much has changed after another 24 hours (Fig. 9), suggesting that they are not able to adequately encourage each other's growth and movement.

3.2. Lactate dehydrogenase (LDH) assay

To be able to understand the LDH assay, a short description of the process must be given. This concept presents an approach where a rupture of the plasma membrane takes place, followed by the spread of the LDH across the supernatant of the cellular culture, which further causes necrosis, apoptosis, or any sort of cell demise.

Further, pyruvate is transformed into lactate, resulting in NADH, which decreases byproducts to quantifiable forms. NADH converts yellow tetrazolium salt (INT), which absorbs at 492 nm, into red, water-soluble formazan. The formazan concentration corresponds to the total number of cells that have died or have been altered. [28]

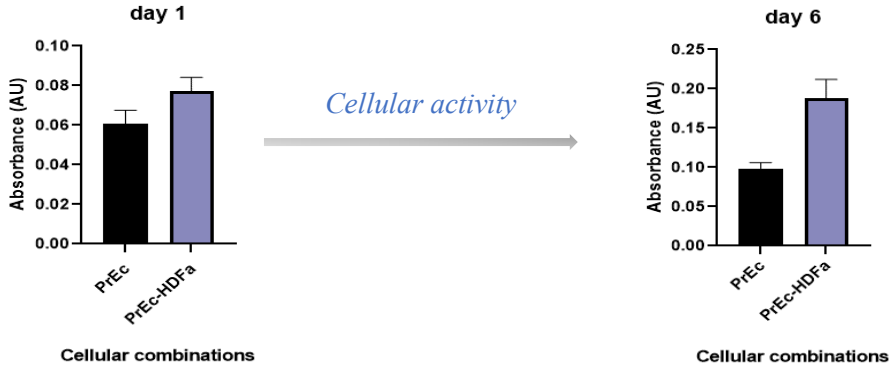

Fig. 10. Cytotoxicity test performed at day 1 and day 6 for the two cellular mixtures.

Recurring to the present study, the LDH cytotoxicity detection kit (Roche) was chosen to assess the cytotoxicity of the samples, and a wavelength standard of 600 nm with NanoQuant Infinite M200 Pro equipment tracked down the activity of LDH in the supernatant.

Moreover, following the initial LDH measure, Fig. 10 depicts that the cellular pairings (exclusive PrEc; PrEc-HDFa) have decent rates of survival along with results that do not differ significantly regardless of the variance of cellular lines. This pattern persisted in culture throughout the entire period.

Nevertheless, the LDH levels in the PrEC samples were low, partially attributed to the slow proliferation rate of the cells. Ultimately, the formazan concentration in the cell culture corresponds to the total amount of cells that died or were altered.

3.3. Fluorescence microscopy test.

To investigate biocompatibility, the fluorescent live-death test was carried out, which involved labeling living cells green with calcein and dead cells red with an ethidium bromide-intercalating dye and observing them under a Zeiss Axio Vert A1 microscope. Skin fibroblasts and intestinal epithelial cells were also examined to determine the ideal conditions for proliferation, migration, and tissue development.

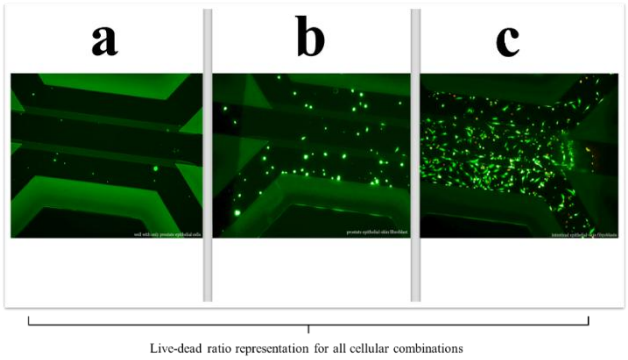

Fig. 11. Well comparison in channels: a. prostate epithelial cells exclusively; b. prostate epithelia combined with skin fibroblast; c. intestinal epithelia combined with skin fibroblasts.

The overall cellular activity within the well for each cell pairing using this approach can be seen in Fig. 11.

Beyond that, in the well exclusively with PrEc, there is less contact and proliferation in contrast to PrEc-HDFa and IEc-HDFa, even though their live-to-dead ratios of cells are alike.

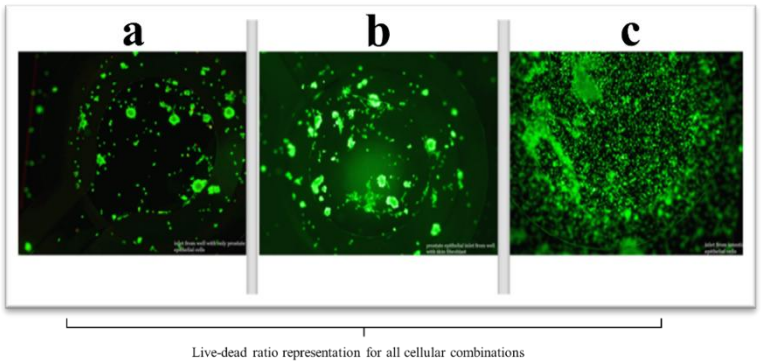

Fig. 12. Well comparison at the inlets: a. prostate epithelial cells exclusively; b. prostate epithelia combined with skin fibroblast; c. intestinal epithelia combined with skin fibroblasts.

When the PrEc underwent investigation with HDFa, a similar interaction between fibroblasts and epithelia was revealed as it would with a constantly developing cancerous IEc. The latter result arises by heading to the inlet of every arrangement and finding which cells in the exclusive PrEc well have slight changes (Fig. 12).

Accordingly, if PrEc is involved with stromal cells (because of their affinity towards them in the prostate), there will likely be noticeable changes in the OrganoPlate. Nevertheless, because of this, PrEc cannot develop by itself and rather evolves gradually when it interacts with other cellular lines.

4. Conclusions

Throughout the entire study, several tests were performed to demonstrate the inability of prostate epithelial cells to grow and differentiate without the presence of specific complementary lines required in a healthy human prostate.

For this, phase contrast microscopy, lactate dehydrogenase (LDH) assay, and fluorescence microscopy were employed, and the results confirmed this. Not only did the cells fail to grow and differentiate properly, but they also showed limited migration, with most remaining near the entrance of the well and only a few reaching the central interaction area.

Moreover, the LDH assay indicated that only in the presence of fibroblasts was there a significant enhancement of epithelial adhesion and proliferation, suggesting that epithelial cells differentiate most effectively alongside their natural stromal partners. Lastly, although the live-to-dead ratio was similar across all conditions, wells with only epithelial cells exhibited reduced growth and minimal interaction.

These findings suggest that the co-cultured MIMETAS model could be useful for personalized medicine approaches in prostate cancer. Replicating native stromal-epithelial interactions may aid in better modeling patient-specific tumor microenvironments and, potentially, inform therapeutic strategies.

Acknowledgements

This research study was supported by a National Research Grant - ARUT, contract no. 23/09.10.2023, *New smart hydrogels based on biopolymers and graphene oxide for photothermal therapy*.

REFERENCES

[1] G. L. Varaprasad et al., “Recent advances and future perspectives in the therapeutics of prostate cancer,” Experimental Hematology & Oncology 2023 12:1, vol. 12, no. 1, pp. 1–24, Sep. 2023, doi: 10.1186/S40164-023-00444-9.

[2] K. L. Ng, “The Etiology of Prostate Cancer,” Prostate Cancer, pp. 17–28, May 2021, doi: 10.36255/EXONPUBLICATIONS.PROSTATECANCER.ETIOLOGY.2021.
[3] “FDA Drug Safety Communication: 5-alpha reductase inhibitors (5-ARIs) may increase the risk of a more serious form of prostate cancer | FDA.” Accessed: Apr. 20, 2023. [Online]. Available: https://www.fda.gov/drugs/drug-safety-and-availability/fda-drug-safety-communication-5-alpha-reductase-inhibitors-5-aris-may-increase-risk-more-serious
[4] A. R. Rao, H. G. Motiwala, and O. M. A. Karim, “The discovery of prostate-specific antigen,” BJU Int., vol. 101, no. 1, pp. 5–10, Jan. 2008, doi: 10.1111/J.1464-410X.2007.07138.X.
[5] G. Shaw and R. Almeida-Magana, “Prostate cancer diagnosis, classification and treatment overview,” Surgery (Oxford), vol. 43, no. 10, pp. 648–656, Oct. 2025, doi: 10.1016/J.MPSUR.2025.07.016.
[6] J. Griffith and L. Wiegand, “Literature review on the efficacy of treatments for urinary incontinence in irradiated vs. non-radiated men treated for prostate cancer,” AME Med. J., vol. 7, no. 0, Sep. 2022, doi: 10.21037/AMJ-22-5/COIF.
[7] R. J. Rebello et al., “Prostate cancer,” Nature Reviews Disease Primers 2021 7:1, vol. 7, no. 1, pp. 1–27, Feb. 2021, doi: 10.1038/s41572-020-00243-0.
[8] “Development, Molecular Biology, and Physiology of the Prostate | Abdominal Key.” Accessed: Apr. 04, 2024. [Online]. Available: https://abdominalkey.com/development-molecular-biology-and-physiology-of-the-prostate/
[9] D. Vecchiotti et al., “Evidence of the Link between Stroma Remodeling and Prostate Cancer Prognosis,” Cancers (Basel)., vol. 16, no. 18, p. 3215, Sep. 2024, doi: 10.3390/CANCERS16183215.
[10] Y. N. Niu and S. J. Xia, “Stroma–epithelium crosstalk in prostate cancer,” Asian J. Androl., vol. 11, no. 1, p. 28, 2009, doi: 10.1038/AJA.2008.39.
[11] L. Jiang et al., “Human stroma and epithelium co-culture in a microfluidic model of a human prostate gland,” Biomicrofluidics, vol. 13, no. 6, Nov. 2019, doi: 10.1063/1.5126714.
[12] L. Jiang, H. Khawaja, S. Tahsin, T. A. Clarkson, C. K. Miranti, and Y. Zohar, “Microfluidic-based human prostate-cancer-on-chip,” Front. Bioeng. Biotechnol., vol. 12, p. 1302223, Jan. 2024, doi: 10.3389/FBIOE.2024.1302223/PDF.
[13] D. E. Ingber, “Human organs-on-chips for disease modelling, drug development and personalized medicine,” Nature Reviews Genetics 2022 23:8, vol. 23, no. 8, pp. 467–491, Mar. 2022, doi: 10.1038/s41576-022-00466-9.
[14] J. E. Sosa-Hernández et al., “Organs-on-a-Chip Module: A Review from the Development and Applications Perspective,” Micromachines (Basel)., vol. 9, no. 10, Oct. 2018, doi: 10.3390/MI9100536.
[15] N. Del Piccolo et al., “Tumor-on-chip modeling of organ-specific cancer and metastasis,” Adv. Drug Deliv. Rev., vol. 175, p. 113798, Aug. 2021, doi: 10.1016/J.ADDR.2021.05.008.
[16] “Asses Cell Migration In Vitro In a 3D Tumor Microenvironment.” Accessed: Oct. 24, 2025. [Online]. Available: https://www.mimetas.com/en/3d-cell-migration/
[17] C. H. Park, J. H. Park, and Y. J. Suh, “Perspective of 3D culture in medicine: transforming disease research and therapeutic applications,” Front. Bioeng. Biotechnol., vol. 12, p. 1491669, 2024, doi: 10.3389/FBIOE.2024.1491669.
[18] L. Jiang, H. Khawaja, S. Tahsin, T. A. Clarkson, C. K. Miranti, and Y. Zohar, “Microfluidic-based human prostate-cancer-on-chip,” Front. Bioeng. Biotechnol., vol. 12, p. 1302223, Jan. 2024, doi: 10.3389/FBIOE.2024.1302223/PDF.
[19] L. Jiang et al., “Human stroma and epithelium co-culture in a microfluidic model of a human prostate gland,” Biomicrofluidics, vol. 13, no. 6, p. 064116, Nov. 2019, doi: 10.1063/1.5126714.
[20] “Microfluidics Module User’s Guide,” 1998.

[21] A. B. Yasunaga, Y. Murad, V. Kapras, F. Menard, and I. T. S. Li, "Quantitative interpretation of cell rolling velocity distribution," Biophys. J., vol. 120, no. 12, p. 2511, Jun. 2021, doi: 10.1016/J.BPJ.2021.04.021.

[22] R. Fu et al., "Type III Collagen Promotes Pseudopodium-Driven Cell Migration," Chem & Bio Engineering, vol. 2, no. 2, pp. 97–109, Feb. 2024, doi: 10.1021/CBE.4C00133.

[23] Y. Yin, S. L. Waters, and R. E. Baker, "The influence of cell phenotype on collective cell invasion into the extracellular matrix," Oct. 2025, Accessed: Oct. 24, 2025. [Online]. Available: https://arxiv.org/pdf/2506.06810v1

[24] "CFD Module User's Guide," 1998, Accessed: Oct. 24, 2025. [Online]. Available: www.comsol.com/blogs

[25] N. Gilani, P. Malcolm, and G. Johnson, "A model describing diffusion in prostate cancer," Magn. Reson. Med., vol. 78, no. 1, pp. 316–326, Jul. 2017, doi: 10.1002/MRM.26340.

[26] © C Robert Bagnell and F. Zernike, "Chapter 10 Phase Contrast Types of Specimens for Phase Contrast Historical Background of Phase Contrast".

[27] M. S. Kang, H. R. Kim, and M. H. Kim, "Cell classification in 3D phase-contrast microscopy images via self-organizing maps," Lecture Notes in Computer Science (including subseries Lecture Notes in Artificial Intelligence and Lecture Notes in Bioinformatics), vol. 8888, pp. 652–661, 2014, doi: 10.1007/978-3-319-14364-4_63/COVER.

[28] P. Kumar, A. Nagarajan, and P. D. Uchil, "Analysis of Cell Viability by the Lactate Dehydrogenase Assay," Cold Spring Harb. Protoc., vol. 2018, no. 6, p. pdb.prot095497, Jun. 2018, doi: 10.1101/PDB.PROT095497.